Tribological properties of room temperature fluorinated graphite heat-treated under fluorine atmosphere

Karl Delbé, Philippe Thomas, David Himmel, Jean-Louis Mansot, Marc Dubois, Katia Guérin, Céline Delabarre, André Hamwi

Tribological Properties of Room Temperature Fluorinated Graphite Heat-Treated Under Fluorine Atmosphere

K. Delbé · P. Thomas · D. Himmel · J. L. Mansot · M. Dubois · K. Guérin · C. Delabarre · A. Hamwi

Abstract This work is concerned with the study of the tribologic properties of room temperature fluorinated graphite heat-treated under fluorine atmosphere. The fluorinated compounds all present good intrinsic friction properties (friction coefficient in the range 0.05–0.09). The tribologic performances are optimized if the materials present remaining graphitic domains (influenced by the presence of intercalated fluorinated species) whereas the perfluorinated compounds, where the fluorocarbon layers are corrugated (armchair configuration of the saturated carbon rings) present higher friction coefficients. Raman analyses reveal that the friction process induces severe changes in the materials structure especially the partial rebuilding of graphitic domains in the case of perfluorinated compounds which explains the improvement of μ during the friction tests for these last materials.

Keywords Friction · Fluorinated carbons · Raman spectroscopy

1 Introduction

Conventional fluorocarbon materials CF_x are generally prepared by direct reaction of fluorine with carbon materials. A reaction temperature above 350 °C is needed if graphite is used as the starting material. Such compounds are characterized by puckered fluorocarbon layers (armchair conformation) associated to covalent C–F bonds. In these structures carbon atoms present a sp^3 hybridization [1]. These fluorinated compounds are used both as cathode materials in lithium batteries [2, 3] and as solid lubricants [4–6].

The fluorination of graphite is also possible at room temperature in the presence of catalysts [7, 8], such as volatile inorganic fluoride and gaseous HF [9]. The obtained fluorinated materials, in which the planarity of the graphene layers is maintained (sp^2 hybridization of the carbon atoms) and the character of the C–F bonds is semi-ionic, present good electrochemical properties [10].

Recently, graphite fluorides obtained at room temperature by the reaction of graphite with gaseous F_2, HF, and MF_n mixture (the volatile fluorides MF_n used were IF_5, BF_3, and ClF_3) have been treated under fluorine at temperatures between 100 and 600 °C [11–15]. The coexistence of sp^2 and sp^3 carbon atoms confers to these materials interesting electrochemical properties for primary lithium batteries [16]. We showed in a previous work that the compounds obtained in the case of F_2, HF, and IF_5 mixture present rather good tribologic properties, influenced by the nature of the C–F bonds, the presence of intercalated species and the fluorine content [17].

The aim of the present work is to investigate the tribologic behavior of room temperature fluorinated graphite and to determine the predominant parameters involved in the improvement of the friction performances. The tribological studies are completed by Raman spectroscopy analyses of the final tribofilm in order to point out the structural evolutions undergone by the tested materials during the friction process.

K. Delbé · P. Thomas (✉) · D. Himmel · J. L. Mansot
Groupe de Technologie des Surfaces et Interfaces (GTSI), EA 2432, Faculté des Sciences Exactes et Naturelles, Université des Antilles et de la Guyane, 97159 Pointe à Pitre Cedex, France
e-mail: Philippe.Thomas@univ-ag.fr

M. Dubois · K. Guérin · C. Delabarre · A. Hamwi
Laboratoire des Matériaux Inorganiques, UMR CNRS-6002, Université Blaise Pascal de Clermont-Ferrand, 63177 Aubière, France

2 Experimental

2.1 Materials

Fluorinated graphites are prepared from Madagascar natural graphite powder at room temperature in a F_2 atmosphere with a gaseous mixture of HF and a volatile inorganic fluoride to improve the reactivity of fluorine with graphite [10]. The volatile fluorides MF_n used are BF_3 and ClF_3, leading to the fluorinated materials noted B and C, respectively. The reaction time is 14 h. The synthesis method is precisely described elsewhere [14, 15]. The compounds are then treated under fluorine atmosphere at temperatures, noted T_{FPT}, ranging from 150 to 600 °C leading to two series of compounds, named B(T_{FPT}) and C(T_{FPT}).

2.2 Tribologic Tests

The tribologic properties of the compounds are evaluated using an alternative ball-on-plane tribometer, the ball motion being a backward and forward motion on the static plane.

Balls are used as delivered while planes are polished to obtain a roughness needed to improve the adherence of the tested tribofilm. Surface characterizations are performed with an optical Altisurf 500 profilometer, allowing to evaluate surface profiles with a resolution of 10 nm and to determine 2D (R_a) and 3D (S_a) roughness parameters. The metallurgical characteristics and typical roughness data of both balls and planes as well as the tribologic test conditions are summarized in Table 1. After ultrasonic cleaning in ethanol and acetone, the solid lubricant is deposited on the plane by the burnishing technique. The procedure is the following: a few milligrams of the compound is deposited on the plane. Then a second plane is used to apply by crushing the powder on the rough surface leading to an adherent film of 1–2 μm thickness and 5 mm^2 area on each plane.

The friction coefficient is measured under air atmosphere (relative humidity: 50–55%), with a computer-based data acquisition system:

The values of friction coefficient measured after three cycles is considered to correspond to the intrinsic tribologic properties of the deposited film.

The values recorded after 30, 100, 200, and 500 cycles will allow us to point out possible friction properties evolution induced by the transformations of the initial materials during the friction process.

2.3 Raman Investigations

Raman spectroscopy analyses of the initial compounds and of the tribofilms at the end of the friction tests are performed using a HR 800 Horiba multi channel spectrometer fitted with a Peltier cooled CCD detector for signal recording. The exciting monochromatic light used is the 532 nm wavelength line delivered by a solid Nd YAG laser. The pre-monochromator is a notch filter and the monochromator a 300 lines/mm holographic grating. In our conditions (objective lens ×50, confocal hole 500 μm, spectrometer entry aperture 500 μm), the probe diameter is of 7 μm, the wavenumber resolution is of 1.5 cm^{-1} and dispersion 0.75 cm^{-1}/pixel. The laser power at the sample level is 30 mW and the acquisition time is in the range of 10–60 s depending on the sample thickness. Special attention is paid to avoid sample irradiation damages during the analyses. In order to determine with a high precision Raman bandshifts due to structure evolutions, the sample are simultaneously illuminated with a vapor mercury lamp. The emitted lines appearing at 1464 and 1527 cm^{-1} are used as internal spectra references, the band position being deduced with a precision of ±1 cm^{-1}.

Table 1 Experimental parameters of the tribologic tests

Steel ball	Metallurgy AISI 52100
	HV = 850
	Reduced Young modulus $E^* = 115$ GPa
	Diameter: 9.5 mm
	Roughness: $R_a = 90 \pm 10$ nm
	$S_a = 120$ nm
Steel plane	Metallurgy AISI 52100
	HV = 850
	Reduced Young modulus $E^* = 115$ GPa
	Diameter: 10 mm
	Roughness: $R_a = 350 \pm 10$ nm
	$S_a = 405$ nm
Normal load	10 N
Contact diameter (Hertz's theory)	140 μm
Mean contact pressure	0.65 GPa
Sliding speed	6 mm s^{-1}

According to Hertz' theory, the contact diameter a is given by the relation: $a = \left(\frac{3F_nR*}{4E*}\right)^{1/3}$, where F_n is the applied normal load, R^* the radius of the ball, and E^* the reduced Young modulus ($E^* = 115$ GPa)

3 Results

3.1 Structural Evolution of Fluorinated Graphite as a Function of the Fluorination Post-Treatment Temperature

The evolutions of the chemical composition and of the interlayer distance d_{001} of fluorinated graphites B(T_{FPT})

Table 2 Evolution of the fluorine content (expressed as atomic F/C ratio determined from weight uptake [14, 15]) and interlayer spacing (deduced from XRD patterns [14, 15]) as a function of fluorination post-treatment temperature T_{FPT} for B (synthesized with F_2–HF–BF_3 gaseous mixture) and C (synthesized with F_2–HF–ClF_x gaseous mixture) series

Fluorination post-treatment temperature (T_{FPT}) (°C)	B series		C series	
	F/C ratio	d_{001} (nm)	F/C ratio	d_{001} (nm)
Room temperature	0.47	0.629	0.42	0.626
150	0.39	0.617	–	–
250	0.40	0.620	0.41	0.623
300	0.41	0.621	0.43	0.630
350	0.63	0.621	0.45	0.632
400	0.85	0.655	0.51	0.643
450	0.93	0.701	0.80	0.693
500	0.99	0.734	0.93	0.718
550	1.01	0.702	0.94	0.720

Fluorine contents correspond to both intercalated fluorinated species (HF, MF_n, etc.) and fluorine atoms bonded to carbon layers. F/C ratio remains stable for moderate T_{FPT}s due to progressive transformation of intercalated species and moderate fluorination of carbon layers. For 350 °C < T_{FPT}s < 450 °C, the increase of F/C ratios is associated to the progressive elimination of intercalated species and increase of fluorine atoms covalently bonded to carbon atoms. For T_{FPT}s > 450 °C, intercalated fluorinated species have been totally removed from the host structure and all the carbon atoms are fluorinated

and C(T_{FPT}) are given in Table 2. The fluorination content (expressed as F/C ratio) was calculated by considering the weight uptake of fluorine and the initial weight of graphite. This method is based on the increase of the weight of the sample during the fluorination process. The evaluation of this weight uptake attributed to fluorine allows us to determine the stoichiometry of the compounds and consequently the F/C ratio.

The structural characterization reveals that the compounds obtained at room temperature are stage 1 GICs in which fluorine but also MF_n and HF_n species are intercalated between the graphene sheets [14, 15]. The thermal post-treatment under fluorine atmosphere of the GICs obtained at room temperature will induce important structure evolutions depending on T_{FPT}. For intermediate post-treatment temperatures (150 °C < T_{FPT} < 450 °C), the graphitic structure is still maintained. When the fluorination post-treatment temperature is increased, the intercalated species are progressively eliminated from the van der Waals gaps and covalent C–F bonds, associated to a sp^3 hybridization of the carbon atoms, are formed. The materials appear biphasic:graphitic microdomains (planar shape of the carbon sheets associated to a sp^2 hybridization of the carbon atoms) coexist with puckered fluorocarbon layers domains. The structure evolution as a function of T_{FPT} and of F/C ratio and composition is given in Tables 3 and 4 for B and C series, respectively. The idealized structures are schematically presented in Fig. 1. For the highest T_{FPT}s (above 500 °C), the armchair structure extends over the whole material. These structural evolutions result in a modification of the interlayer spacing d_{001} as revealed by the linear relationship between the d_{001} enhancement and the F/C ratio (Fig. 2) which lead to interlayer interactions changes and probably influence the tribologic properties of the fluorinated compounds.

3.2 Intrinsic Tribologic Properties of Graphite Fluorides

The friction coefficients obtained for the various fluorinated materials at the beginning of the tribological test (3 cycles) are presented in Fig. 3 as a function of fluorination post-treatment temperature. All the compounds present good intrinsic friction properties, better than pristine graphite. The lowest friction coefficients are obtained for low and intermediate fluorination temperatures as μ remains in the same range ($\mu = 0.055$ and $\mu = 0.06$ for B and C series, respectively) for initial compounds and materials post-treated up to 450 °C. An increase of μ is observed for T_{FPT}s > 500 °C (0.09 and 0.1 for B and C materials, respectively).

In order to identify the predominant parameters involved in the friction reduction process, correlations between friction coefficient, atomic F/C ratio and interlayer spacing d_{001} are presented in Fig. 2. The results indicate that the intrinsic friction coefficient is low and stable (around 0.06) for a large range of F/C ratios (0.3 < F/C < 0.9), associated to d_{001} values in the range 0.6–0.7 nm and that the fluorinated compounds characterized by the highest F/C ratios (above 0.9) or d_{001} values (above 0.7 nm) exhibit the worse intrinsic tribologic behavior ($\mu > 0.07$). In these materials, all the carbon–fluorine bonds are covalent and the structure is characterized by puckered fluorocarbon layers (armchair conformation). The best tribological results are observed for compounds presenting graphitic or biphasic structures (see Tables 3 and 4). This confirms that the fluorine content and the interlayer distance expansion are not relevant parameters to explain the friction reduction properties of the tested materials.

Raman spectroscopy analyses were performed on the tested materials before the friction tests to correlate the structure to the tribological performances. The spectra recorded on B(T_{FPT}) and C(T_{FPT}) compounds are given in Figs. 4 and 5, respectively in the wave number range 1000–1800 cm^{-1}. The solid lines shown at 1350 and 1580 cm^{-1} indicate the position of the Raman bands corresponding to the D and G bands classically observed in the

Table 3 Evolution of the nature of intercalated species, the nature of the C–F bond and the corresponding hybridization of the carbon atoms and F/C ratio as a function of the fluorination post-treatment temperature for B(T_{FPT}) compounds

Fluorination post-treatment temperature	Intercalated species	Nature of C–F bond	Fluorine content
Room temperature	BF_3 + BF_4^- HF_n(HF, HF_2^-)	Semi-ionic (Csp^2)	F/C = 0.47
100 °C < T_{FPT} < 250 °C	BF_3 ↘ + BF_4^- ↗	Semi-ionic (Csp^2)	F/C ≈ 0.40
	HF_2^- ↘		
250 °C < T_{FPT} < 350 °C	BF_4^- ↘	Semi-ionic (Csp^2)	0.40 < F/C < 0.63
	HF_2^- ↘		
350 °C < T_{FPT} < 500 °C	BF_4^- ↘	Semi-ionic + covalent (Csp^2 + Csp^3)	0.63 < F/C < 0.99
T_{FPT} > 500 °C	None	Covalent (Csp^3)	F/C ≈ 1

For Room temperature < T_{FPT}s < 350 °C, the structure of the compound is graphitic (stage 1 GIC). Fluorinated species remain intercalated and fluorine atoms are semi-ionically bonded to graphene planes. For 350 °C < T_{FPT}s < 500 °C, the structure becomes biphasic due to the partial and progressive elimination of intercalated species leading to the appearance of fluorine atoms covalently bonded to carbon atoms (armchair configuration of carbon cycles). For T_{FPT}s > 500 °C, intercalated species are totally eliminated from the host structure and fluorine atoms are covalently bonded to carbon atoms

Table 4 Evolution of the nature of intercalated species, the nature of the C–F bond and the corresponding hybridization of the carbon atoms and F/C ratio as a function of the fluorination post-treatment temperature for C(T_{FPT}) compounds

Fluorination post-treatment temperature	Intercalated species	Nature of C–F bond	Fluorine content
Room temperature	$ClHF^-$ HF_n(HF, HF_2^-)	Semi-ionic (Csp^2)	F/C = 0.42
100 °C < T_{FPT} < 350 °C	$ClHF^-$ ↘	Semi-ionic (Csp^2)	0.40 < F/C < 0.45
	HF_2^- ↘		
350 °C < T_{FPT} < 450 °C	HF_2^- ↘	Semi-ionic + covalent (Csp^2 + Csp^3)	0.45 < F/C < 0.80
T_{FPT} > 500 °C	None	Covalent (Csp^3)	F/C ≈ 0.95

For Room temperature < T_{FPT}s < 350 °C, the structure of the compound is graphitic (stage 1 GIC), where fluorinated species are intercalated between the carbon layers and fluorine atoms are semi-ionically bonded to carbon atoms. For 350 °C < T_{FPT}s < 450 °C, the structure is biphasic due to the partial and progressive elimination of intercalated species leading to the appearance of fluorine atoms covalently bonded to carbon atoms (armchair configuration). For T_{FPT}s > 500 °C, intercalated species have been totally eliminated from the host structure leading to fluorine atoms in covalent interaction with carbon atoms

Raman spectrum of graphite [18–20]. The G band is attributed to the optical E_{2g} mode of the carbon atoms and the D mode is associated to disorder. This mode is generally accompanied by another one, noted D′, appearing at 1620 cm^{-1} [20]. The Raman spectra of B(T_{FPT}) and C(T_{FPT}) compounds (Figs. 4 and 5) exhibit the D peak near 1350 cm^{-1} and a composite one near 1600 cm^{-1} resulting from the overlap of the G and D′ modes. The Raman spectra recorded on B(500) and B(550) materials do not exhibit the D and G peaks underlining the absence of aromatic groups in these compounds. It indicates that the structure is totally composed of puckered fluorocarbon layers (the carbon atoms only present sp^3 hybridization). From T_{FPT} = 150–450 °C, spectra show a downshift of the D (and probably D′) band attributed both to electronic effect of fluorine and increase of disorder as already mentioned in previous works [17, 21–24]. The fact that the fluorination of carbon is completed for B(500) and B(550) materials (covalent C–F bonds resulting in the armchair conformation of carbon rings) which present the highest friction coefficient values seems to confirm that the friction properties of the compounds are improved if the graphitic structure is partially maintained. The size reduction of the graphitic domains (L_a coherence length) can be evaluated from the intensities of the D and G Raman bands according to Knight and White relation [25]: $L_a = 44\frac{I_G}{I_D}$. The evolution of L_a as a function of F/C is given in Fig. 6. As already described in the literature, the fluorination process is associated to a drastic reduction of the size of well-ordered graphitic domains even at room temperature, as L_a = 25 and 30 Å for, respectively, initial B and C compounds compared to 100 Å for initial pristine graphite. Then the

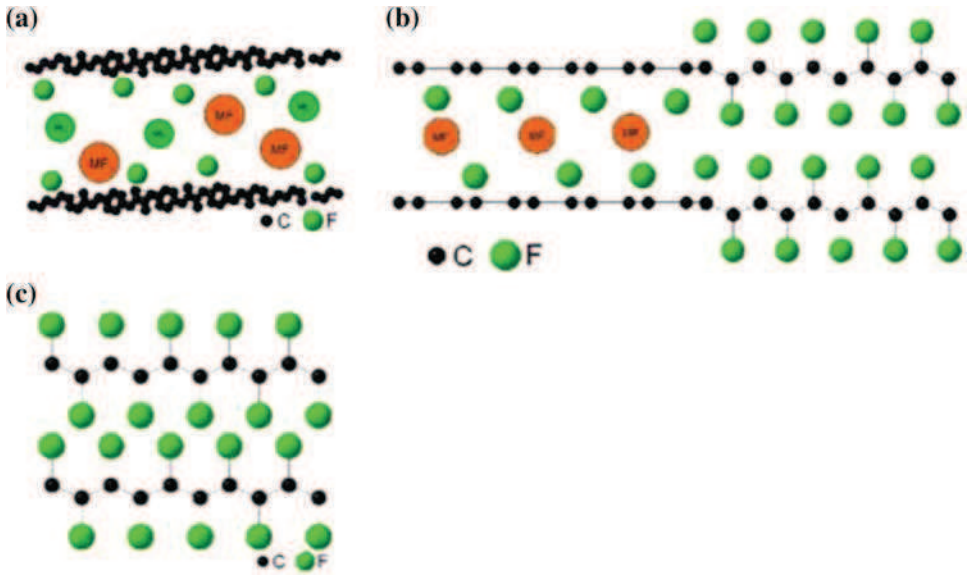

Fig. 1 Idealized representation of the structures of the fluorinated compounds: **a** graphitic (Room temperature < T_{FPT}s < 350 °C), **b** biphasic (350 °C < T_{FPT}s < 450 °C), and **c** armchair structures (T_{FPT}s > 500 °C)

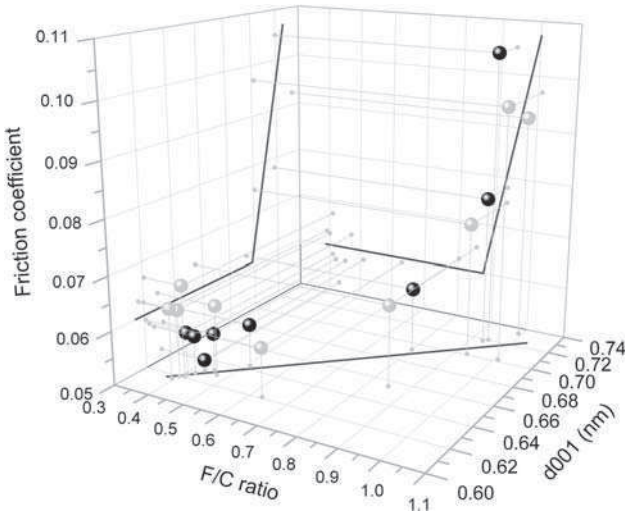

Fig. 2 3D representation of the evolution of the intrinsic friction coefficient as a function of F/C ratio (determined from weight uptake [14, 15]) and corresponding d_{001} spacing (determined from X-ray diffraction patterns [14, 15]) for ○ B(T_{FPT}) compounds and ● C(T_{FPT}) compounds. The projections of the 3D curve on the μ vs. F/C, μ vs. d_{001} and F/C vs. d_{001} planes represent the corresponding evolutions. As it can be seen, d_{001} enhancement is linearly related to the F/C ratio. Consequently, μ present similar evolutions as a function of F/C and d_{001}. These evolutions are characterized by a stability of the friction coefficient in the 0.3 < F/C < 0.9 range and corresponding 0.6–0.7 nm d_{001} range and a drastic increase for F/C > 0.9 (d_{001} > 0.7 nm)

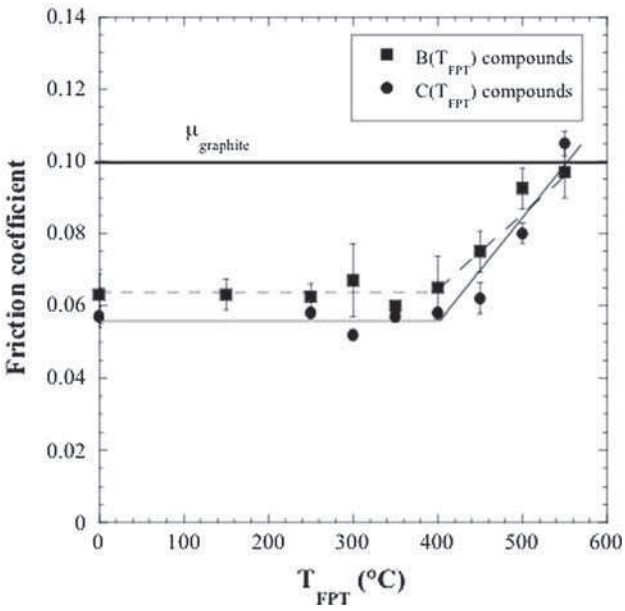

Fig. 3 Evolution of intrinsic friction coefficient (recorded after three cycles) as a function of fluorination post-treatment temperature for B(T_{FPT}) and C(T_{FPT}) materials. The friction coefficient is in the same range (μ = 0.055 and μ = 0.06 for B(T_{FPT}) and C(T_{FPT}) materials, respectively) for Room temperature < T_{FPT}s < 400 °C and increases for T_{FPT}s > 450 °C

influence of fluorination post-treatment is clearly seen in Fig. 6: L_a decreases as a function of the fluorine content for both B and C series to become inferior to 20 Å for F/C ratios above 0.9. The correlation between the friction coefficient and the size of aromatic domains is presented in Fig. 7. The friction coefficient remains stable around 0.06 for graphitic domains size ranging from 20 to 30 Å and increases for lower L_a.

The study of the intrinsic tribologic properties of B(T_{FPT}) and C(T_{FPT}) materials shows that the friction

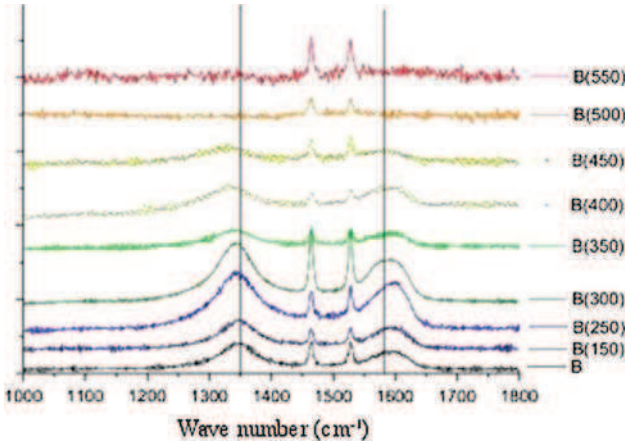

Fig. 4 Raman spectra recorded on B(T_{FPT}) compounds before the friction tests. *Solid lines* correspond to the D (1350 cm^{-1}) and G (1580 cm^{-1}) bands position obtained for graphite [18–20]. The G band is attributed to the optical E_{2g} mode of the carbon atoms and the D mode is associated to disorder. This mode is generally accompanied by another one, noted D′, appearing at 1620 cm^{-1} [20]. The Raman spectra of B(T_{FPT}) compounds exhibit the D peak near 1350 cm^{-1} and a composite one near 1600 cm^{-1} resulting from the overlap of the G and D′ modes. The Raman spectra recorded on B(500) and B(550) materials do not exhibit the D and G peaks underlining the absence of aromatic groups in these compounds. It indicates that the structure is totally composed of puckered fluorocarbon layers (the carbon atoms only present sp^3 hybridization). From $T_{FPT} = 150$ °C to 450 °C, spectra show a downshift of the D band attributed both to electronic effect of fluorine and increase of disorder [17, 21–24]. The two lines appearing at 1464 cm^{-1} and 1527 cm^{-1} are the emission lines of a vapor mercury lamp used as internal standard which allow us to determine precisely the Raman bandshifts in the collected spectra

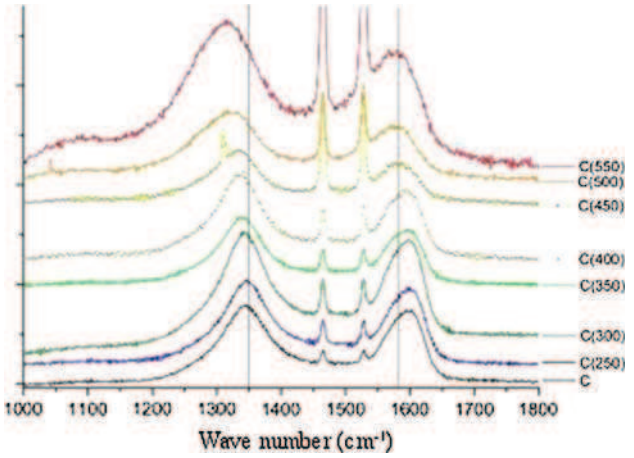

Fig. 5 Raman spectra recorded on C(T_{FPT}) compounds before the friction tests. *Solid lines* correspond to the graphitic D (1350 cm^{-1}) and G (1580 cm^{-1}) bands position. All the Raman spectra exhibit the D band near 1350 cm^{-1} and a composite one near 1600 cm^{-1} resulting from the overlap of the G and D′ modes. This indicates that aromatic rings are present in all materials. The downshift of the D band is attributed both to electronic effect of fluorine and increase of disorder. The two lines appearing at 1464 cm^{-1} and 1527 cm^{-1} are the emission lines of a vapor mercury lamp used as internal standard which allow us to determine precisely the Raman bandshifts in the collected spectra

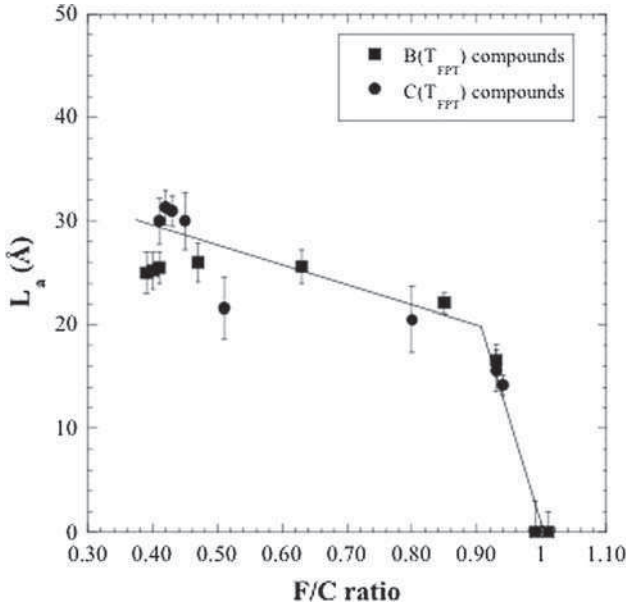

Fig. 6 Evolution of the size of graphitic domains L_a (deduced from Knight and White relation $L_a = 44\frac{I_G}{I_D}$ [25]) as a function of atomic F/C ratio (determined from weight uptake [14, 15]) for B(T_{FPT}) and C(T_{FPT}) materials. The fluorination process is associated to a drastic reduction of the size of graphitic domains ($L_a = 25$ and 30 Å for, respectively, initial B and C compounds compared to 100 Å for initial pristine graphite). L_a decreases as a function of the fluorine content for both B and C series to become inferior to 20 Å for F/C ratios above 0.9

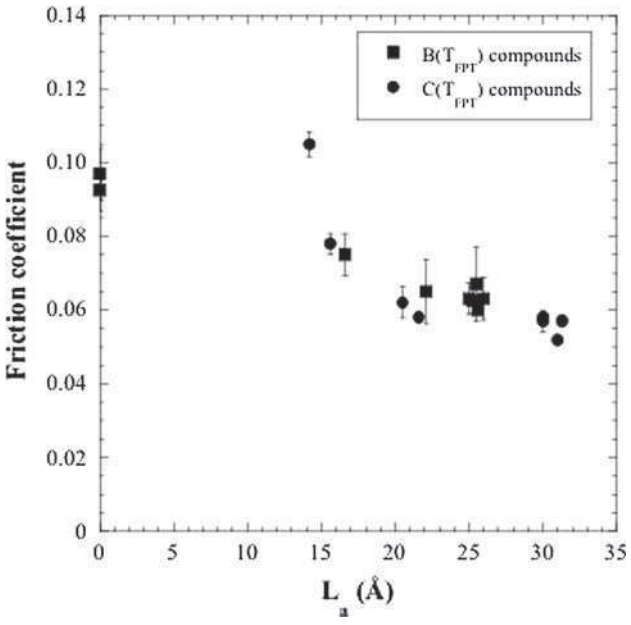

Fig. 7 Evolution of intrinsic friction coefficient (recorded after three cycles) as a function of the size of graphitic domains L_a (deduced from Knight and White relation [25]). The best tribologic properties are obtained for structures presenting significative graphitic domains ($\mu = 0.06$ if the graphitic domains size ranges from 20 to 30 Å) whereas μ increases with increasing armchair configuration contribution

reduction process can not be only related to the fluorine content and the interlayer spacing expansion.

3.3 Influence of the Friction Process on the Tribologic Performances

Figures 8 and 9 present the evolution of the friction properties of B(T_{FPT}) and C(T_{FPT}) compounds as a function of cycles number. The friction coefficient values reported were measured after 3, 30, 100, 200, and 500 cycles. The tribological experiments show a noticeable stability of the performances for low and intermediate T_{FPT}s (μ ranges between 0.055 and 0.065 for B materials and between 0.05 and 0.065 for C compounds) and an improvement of the friction properties for compounds fluorinated above 400 °C as cycles number increases. It must be noted that the decrease of the friction coefficient is observed in the case of materials presenting a biphasic structure or only puckered fluorocarbon layers. This behavior, already observed in the case of graphite fluorides synthesized at room temperature with a gaseous F_2–HF/–IF_5 mixture [17], strongly suggests a structural evolution during the friction test.

In order to confirm this hypothesis, Raman spectroscopy analyses were performed on the phases remaining in the wear scars after 30, 100, 200, and 500 cycles of friction and compared to the spectra recorded on the initial compounds. Figures 10 and 11 present the spectra obtained for initial and post-fluorinated B and C materials, respectively, with fluorination temperatures equal to 250, 350, 450, 500, and 550 °C. All the spectra present the D band at 1348 cm^{-1} and the G + D′ overlap around 1600 cm^{-1}.

The comparison of the spectra collected after 30, 100, 200, and 500 cycles does not emphasize any significant changes of the D and G Raman peaks intensities. In the case of T_{FPT}s < 500 °C, the spectra recorded during the friction tests show an increase of the relative intensities of disorder related D and D′ bands compared to those of initial compounds.

Whereas the D and G Raman bands are not observed in the spectra of the initial B and C compounds post-treated above 500 °C, these bands characteristic of the presence of graphene planes are already revealed in the spectra of the corresponding tribofilms obtained after only 30 cycles. These relative intensities do not evolve for higher cycles number showing the stability of the tribofilm structure. The Raman spectra strongly suggest that friction induces breakings of C–F covalent bonds and partial re-building of graphene planes in the early stages of friction. This phenomenon probably leads to a lowering of interlamellar interactions evidenced by the decrease of the friction coefficient.

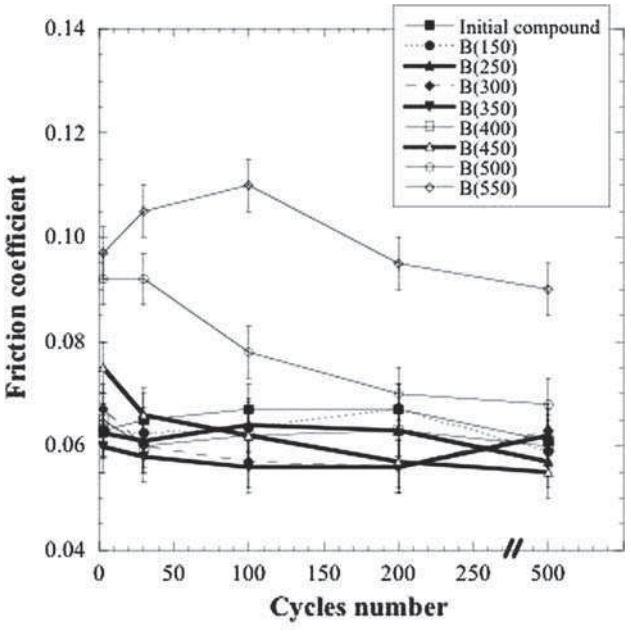

Fig. 8 Evolution of friction coefficient as a function of cycles number for B(T_{FPT}) materials. The friction coefficient was measured at 3, 30, 100, 200, and 500 cycles. The tribological performances are stable for low and intermediate T_{FPT}s ($\mu = 0.06$) whatever the test duration. The friction properties are improved for compounds fluorinated above 400 °C as cycles number increases. These materials present a biphasic or armchair structure. This suggests a structural evolution during the friction test

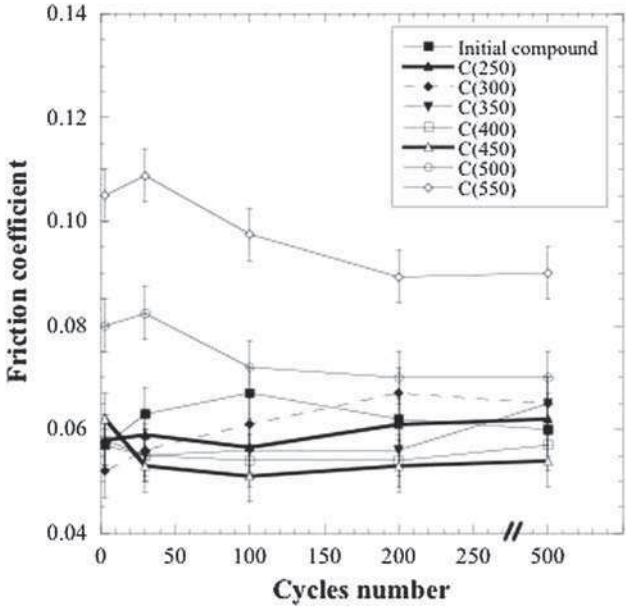

Fig. 9 Evolution of friction coefficient as a function of cycles number (3, 30, 100, 200, and 500 cycles) for C(T_{FPT}) materials. The best tribologic results ($\mu = 0.055$) are obtained for low and intermediate T_{FPT}s. The friction performances are improved with increasing cycles number for materials presenting puckered fluorocarbon layers suggesting a structural evolution during the tribological test

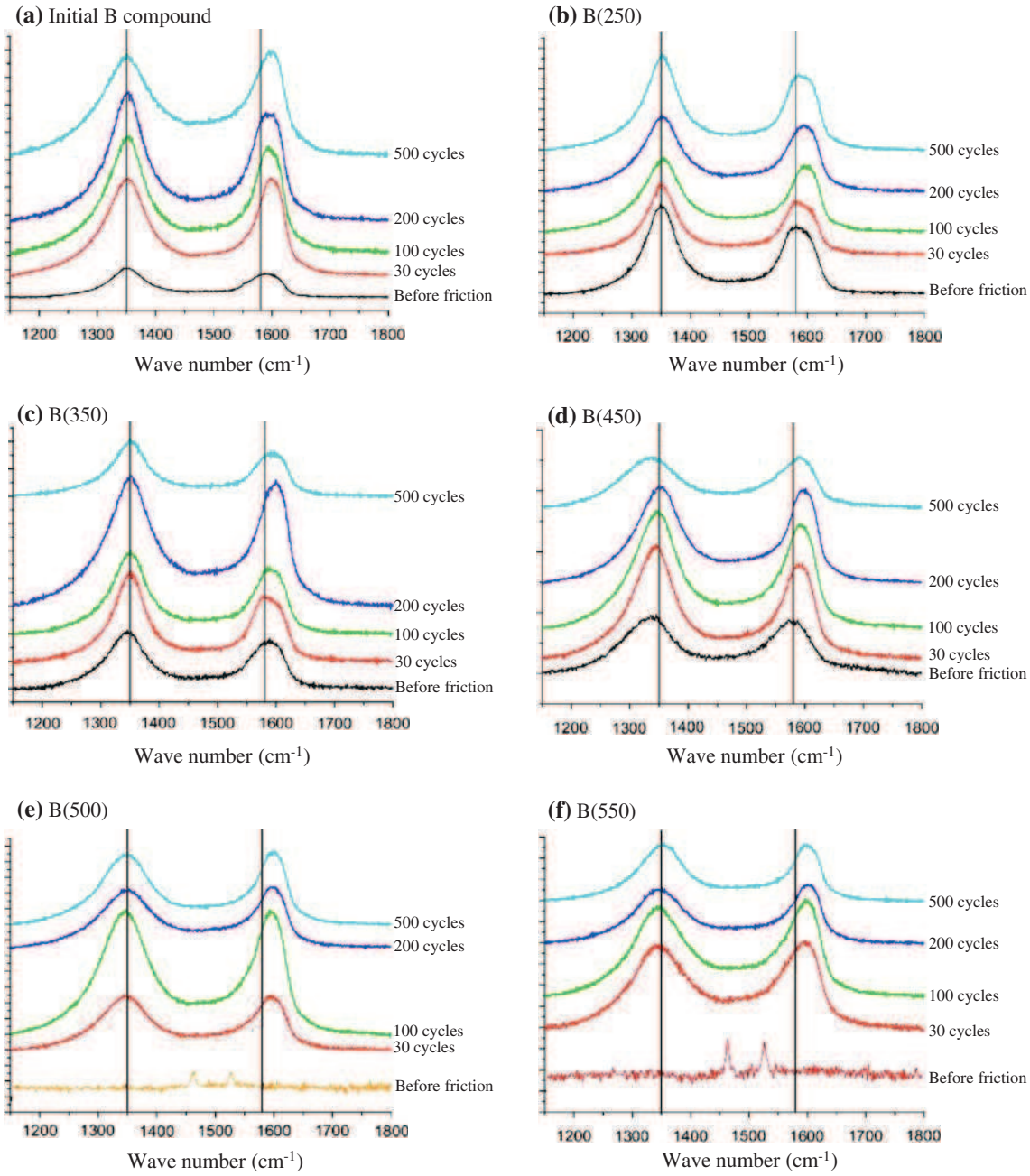

Fig. 10 Raman spectra recorded on initial B(T_{FPT}) compounds before the friction tests and on phases remaining in the wear scar after 30, 100, 200, and 500 cycles, with fluorination temperatures equal to 250, 350, 450, 500, and 550 °C. The spectra all present the D band at 1348 cm^{-1} and the G + D′ overlap around 1600 cm^{-1}, the *solid lines* at 1350 cm^{-1} and 1580 cm^{-1} corresponding to the D and G band positions observed for pristine graphite. For T_{FPT}s < 500 °C, the spectra recorded during the friction tests show an increase of the intensities of disorder related D and D′ bands compared to those of initial compounds. For B(T_{FPT}) materials post-treated above 500 °C, the appearance of the D, G, and D′ bands after friction, whereas no characteristic peaks were observed for initial compounds, shows the presence of graphitic domains resulting from C–F covalent bonds breakings and partial re-building of graphene planes

The similarity of the Raman spectra collected for various cycles numbers is emphasized in Fig. 12 which displays the evolution of L_a coherence length (calculated as previously from I_D/I_G ratio using Knight and White relation [25]) as a function of cycles number in the cases of B(350), B(550), C(350), and C(550) compounds. Whatever the initial size of the graphitic domains are, the friction process leads to an asymptotic value of L_a between 25 and 30 Å.

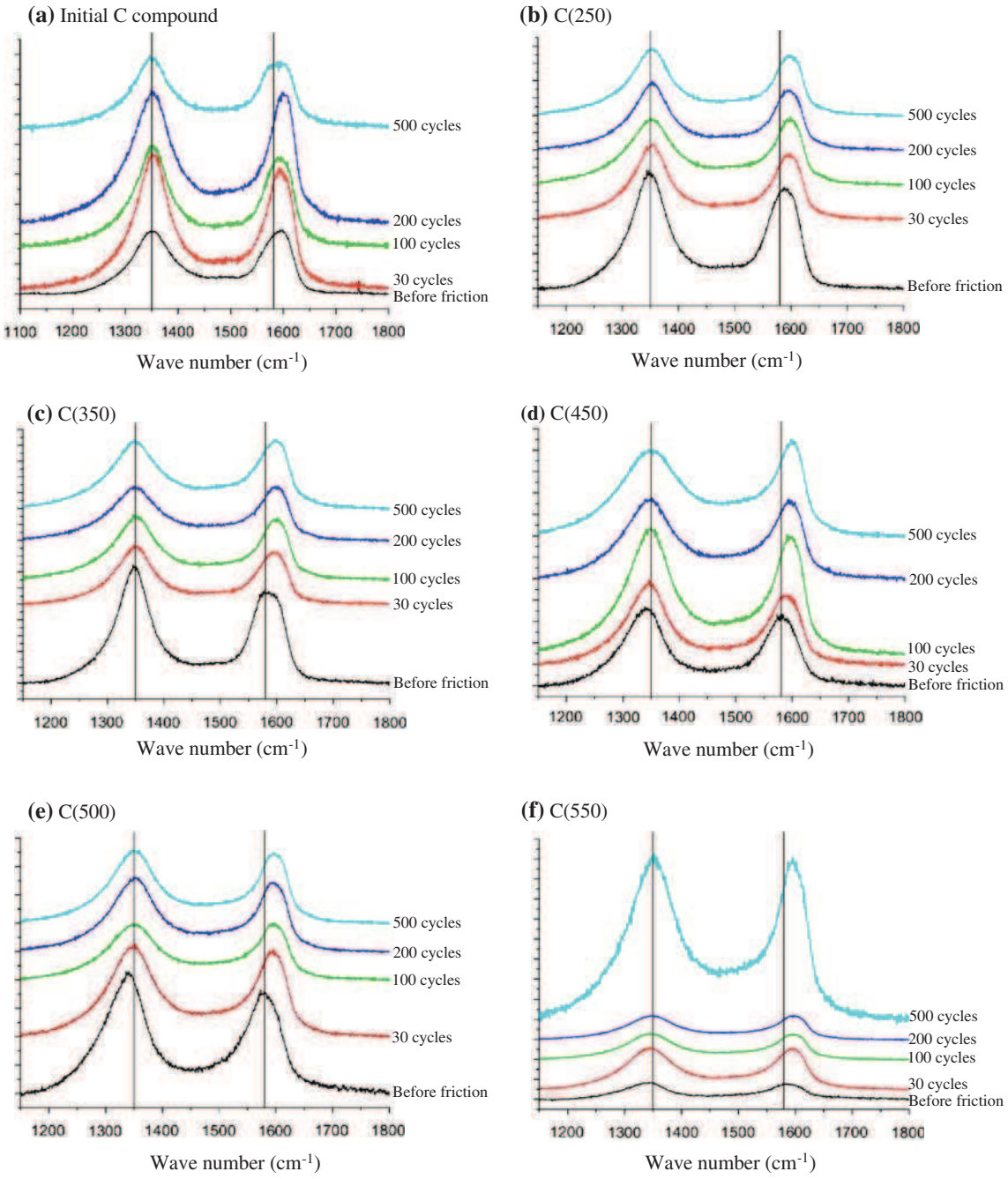

Fig. 11 Raman spectra recorded on C(T_{FPT}) compounds before the friction tests and after 30, 100, 200, and 500 cycles with fluorination temperatures equal to 250, 350, 450, 500, and 550 °C. *Solid lines* correspond the D (1350 cm^{-1}) and G (1580 cm^{-1}) bands position obtained for graphite. The spectra all present the D band at 1348 cm^{-1} and the G + D′ overlap around 1600 cm^{-1}, the solid lines at 1350 cm^{-1} and 1580 cm^{-1} corresponding to the D and G band positions observed for pristine graphite. For T_{FPT}s < 500 °C, the spectra recorded during the friction tests show an increase of the intensities of disorder related D and D′ bands compared to those of initial compounds. For materials post-treated above 500 °C, the increase of the D, G, and D′ bands after friction, compared to the peaks observed for initial compounds, shows an increase of graphitic domains resulting from C–F covalent bonds breakings and partial re-building of graphene planes

4 Discussion

The intrinsic tribologic properties of the tested graphite fluorides clearly demonstrate that the friction reduction process is not directly related to the fluorine content or the fluorination induced interlayer distance expansion as the friction coefficients appear the highest for the greatest F/C ratios and interlayer distances.

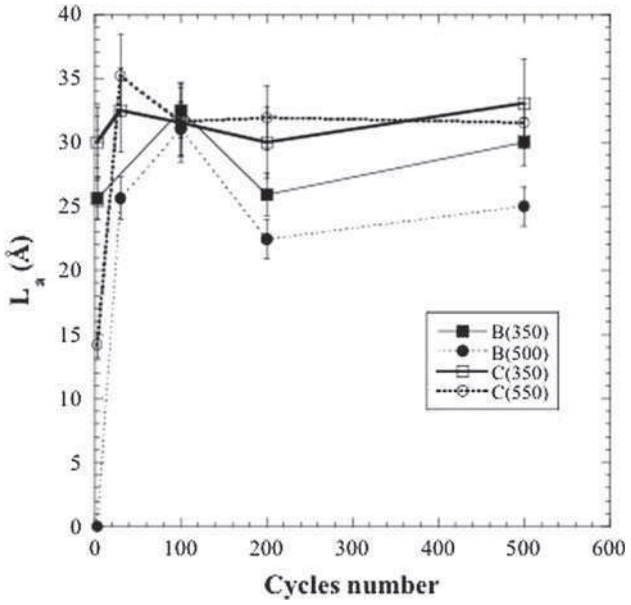

Fig. 12 Evolution of the size of graphitic domains L_a (deduced from Knight and White relation $L_a = 44\frac{I_G}{I_D}$ [25]) as a function cycles number for B(350), B(500), C(350), C(550) materials. Whatever the initial size of the graphitic domains, the friction process leads to an asymptotic value of L_a between 25 and 30 Å

The correlation of the tribologic data to the Raman analyses carried out on the initial compounds points out that low friction coefficients are obtained when a lot of graphene planes are maintained. This corresponds to partially fluorinated compounds (Room Temperature $< T_{FPT} <$ 450 °C), where graphitic domains (fluorine atoms are semi-ionically bonded to aromatic rings) can coexist with perfluorinated ones (fluorine atoms covalently bonded to Csp^3 atoms). The change in the nature of the fluorine–carbon bonding from semi-ionic (planar aromatic graphene layers) to covalent (armchair conformation of non-aromatic carbon rings leading to puckered fluorocarbon layers) leads to a severe evolution of the friction properties. A rapid increase of the friction coefficient is correlated to the increase of C–F covalent bond concentration. This induces a decrease of the graphitic domains extension evidenced by the decrease of L_a (deduced from the Raman spectra) or the disappearance of the Raman graphene bands.

This interpretation is strongly supported by the evolution of the tribologic properties of perfluorinated compounds as a function of the test duration (number of cycles). The experiments clearly show that the improvement of the friction properties are associated to the partial re-building of graphitic domains resulting from C–F bonds breakings induced by the friction process. Effectively, as clearly revealed by the Raman analyses of initial perfluorinated compounds, these ones do not contain any graphene domains as far as the D and G bands characteristic of graphene are no more detected. At the end of the test, the Raman spectra collected on the tribofilms clearly show the D and G bands pointing out the presence of graphene domains in tribofilms. This re-building of these graphene domains needs the elimination of fluorine and restoration of carbon aromatic cycles (C=C bonds). The chemical reaction (C–F bonds breaking) leading to fluorine elimination are tribo-induced reactions. For compounds with $0.3 <$ F/C < 0.9, the stability of the friction coefficient during the long friction tests can be related to the composition and structure stability of the compounds during the tribologic experiment. As for perfluorinated compounds, C–F bonds breakings are also subjected in the partially fluorinated compounds but not pointed out by Raman spectroscopy as far as the technique did not allow us to quantify the amount of fluorine in the tribofilm at the end of the friction tests. However, the large F/C range over which the friction coefficient is stable, as demonstrated by the experimental measurements of the intrinsic properties ($\mu \approx 0.06$ for $0.3 <$ F/C < 0.9), explains the stability of friction during long time testings. Moreover, it must be added that in partially fluorinated compounds, the presence of remaining catalyst molecules and free sites which can trap the free fluorine ions or radicals will participate to the stability of the tribophases composition and structure during friction.

5 Conclusion

The investigation of the tribologic properties of room temperature fluorinated graphite shows a decrease of the friction coefficient, compared to pristine graphite, down to a value close to 0.06 allowing the tested materials to be used as solid lubricants.

Our studies reveal that the lubricating performances are improved if the graphitic structure is significantly maintained in the tested compounds which is achieved in the partially fluorinated materials. The semi-ionic nature of lots of the C–F bonds which maintain the planar shape of the graphene planes and the presence of intercalated fluorinated species which weakly interact with the host matrix in those last compounds favorably participate to the improvement of friction properties.

Long experiments results completed by Raman analyses of the tribofilm lead to the conclusion that the friction process induces a breaking of covalent C–F bonds and a partial re-building of graphitic structure in the perfluorinated compounds leading to an improvement of the tribo-properties of the tribofilm. In the case of partially fluorinated materials, the presence of intercalated fluorides and the semi-ionic nature of lots of C–F bonds allow the released fluorine atoms to be trapped in the structure and/or

to create new C–F bonds and explains the good stability of the tribological performances of the tribofilm.

References

1. Kita, Y., Watanabe, N., Fuji, Y.: Chemical composition and crystal structure of graphite fluoride. J. Am. Chem. Soc. **101**, 3832–3841 (1979)
2. Watanabe, N.: Types of graphite fluorides, $(CF)_n$ and $(C_2F)_n$, and discharge characteristics ans mechanisms of electrodes of $(CF)_n$ and $(C_2F)_n$ in lithium batteries. Solid State Ionics **1**, 87–110 (1980)
3. Nakajima, T.: Carbon-fluorine compounds as battery materials. J. Fluorine Chem. **100**, 57–61 (1999)
4. Fusaro, R.L., Sliney, J.E.: Graphite fluoride (CFx)n—a new solid lubricant. ASLE Trans. **13**, 56–65 (1970)
5. Fusaro, R.L.: Mechanisms of graphite fluoride $(CF_x)_n$ lubrication. Wear **53**, 303–323 (1979)
6. Tsuya, Y.: Tribology of graphite fluorides. In: Nakajima, T. (ed.) Fluorine-carbon and fluoride-carbon materials, pp. 355–380. Marcel Dekker, New York (1995)
7. Rüdorff, W., Rüdorff, G.: Tetrakohlenstoffmonofluorid, eine neue Graphit-Fluor-Verbindung. Chem. Ber. **80**, 417–423 (1947)
8. Nakajima, T., Kawaguchi, M., Watanabe, N.: Ternary intercalation compound of graphite with aluminum fluoride and fluorine. Z. Naturforsch. **36b**, 1419–1423 (1981)
9. Hamwi, A.: Fluorine reactivity with graphite and fullerenes. Fluoride derivatives and some practical electrochemical applications. J. Phys. Chem. Solids **57**, 677–688 (1996)
10. Hamwi, A., Daoud, M., Cousseins, J.C.: Graphite fluorides prepared at room temperature. 1. Synthesis and characterization. Synth. Metals **26**, 89–98 (1988)
11. Dubois, M., Guérin, K., Pinheiro, J.P., Fawal, Z., Masin, F., Hamwi, A.: NMR and EPR studies of room temperature highly fluorinated graphite heat-treated under fluorine atmosphere. Carbon **42**, 1931–1940 (2004)
12. Guérin, K., Pinheiro, J.P., Dubois, M., Fawal, Z., Masin, F., Yazami, R., Hamwi, A.: Synthesis and characterization of highly fluorinated graphite containing sp^2 and sp^3 carbon. Chem. Mater. **16**, 1786–1792 (2004)
13. Giraudet, J., Dubois, M., Guérin, K., Pinheiro, J.P., Hamwi, A., Stone, W.E.E., Pirotte, P., Masin, F.: Solid-state ^{19}F and ^{13}C NMR of room temperature fluorinated graphite and samples thermally treated under fluorine: low-field and high resolution studies. J. Solid State Chem. **178**, 1786–1792 (2005)
14. Delabarre, C., Guérin, K., Dubois, M., Giraudet, J., Fawal, Z., Hamwi, A.: Highly fluorinated graphite prepared from graphite fluoride formed using BF_3 catalyst. J. Fluorine Chem. **126**, 1078–1087 (2005)
15. Delabarre, C., Dubois, M., Guérin, K., Fawal, Z., Hamwi, A.: Room temperature graphite fluorination process using chlorine as catalyst. J. Phys. Chem. Solids **67**, 1157–1161 (2006)
16. Guérin, K., Yazami, R., Hamwi, A.: Hybrid-type graphite fluoride as cathode material in primary lithium batteries. Electrochem. Solid-State Lett. **7**, A159–A162 (2004)
17. Thomas, P., Delbé, K., Himmel, D., Mansot, J.L., Cadoré, F., Guérin, K., Dubois, M., Delabarre, C., Hamwi, A.: Tribological properties of low-temperature graphite fluorides. Influence of the structure on the lubricating performances. J. Phys. Chem. Solids **67**, 1095–1099 (2006)
18. Dresselhaus, M.S., Dresselhaus, G.: Intercalation compounds of graphite. Adv. Phys. **51**, 1–186 (2002)
19. Dresselhaus, M.S., Pimenta, M.A., Ecklund, P.C., Dresselhaus, G.: Raman scattering in fullerenes and related carbon-based materials. In: Weber, W.H., Merlin, R. (eds.) Raman Scattering in Materials Science, pp. 315–364. Springer, New York (2000)
20. Merlin, R., Pinczuk, A., Weber, W.H.: Overview of phonon Raman scattering in solids. In: Weber, W.H., Merlin, R. (eds.) Raman Scattering in Materials Science, pp. 1–29. Springer, New York (2000)
21. Rao, A.M., Fung, A.W.P., di Vittorio, S.L., Dresselhaus, M.S., Dresselhaus, G., Endo, M., Oshida, K., Nakajima, T.: Raman scattering and transmission-electron-microscopy studies of fluorine-intercalated graphite fibers C_xF ($7.8 \geq x \geq 2.9$). Phys. Rev. B **45**, 6883–6892 (1992)
22. Gupta, V., Nakajima, T., Zemva, B.: Raman scattering of higly fluorinated graphite. J. Fluorine Chem. **110**, 145–151 (2001)
23. Gupta, V., Nakajima, T., Ohzawa, Y., Zemva, B.: A study on the formation of graphite fluorides by Raman spectroscopy. J. Fluorine Chem. **120**, 143–150 (2003)
24. Joly-Pottuz, L., Ohmae, N.: Carbon-based nanolubricants. In: Martin, J.M., Ohmae, N. (eds.) Nanolubricants, pp. 93–147.. Tribology SeriesWiley, New York (2008)
25. Knight, D.S., White, W.B.: Characterization of diamond films by Raman spectroscopy. J. Mater. Res. **4**, 385–393 (1989)